


Double Bonds Hot Paper

 How to cite: *Angew. Chem. Int. Ed.* **2025**, *64*, e202422007
 doi.org/10.1002/anie.202422007

An Authentic Al=Si Double Bond

Nasrina Parvin, Ankur, Bernd Morgenstern, and David Scheschkewitz*

Abstract: Aluminatasilenes are the elusive heavier counterparts of the well-known borataalkenes in which the B=C double bond is formally replaced by an Al=Si moiety. We report the isolation of a four-membered anionic AlSi_3 cycle with a bona fide Al=Si double bond, which is obtained by the reaction of 2 eq. of disilenide $\text{Tip}_2\text{Si}=\text{SiTipLi}$ with H_2AlCl (Tip = 2,4,6-triisopropylphenyl). X-ray crystallography, UV/Vis spectroscopy and computational analysis confirm the double bond character with a very short Al–Si bond of 2.283(1) Å and high Wiberg bond index (WBI) of 1.31. Intramolecular C–H activation by the Al=Si bond and the reactions with sulfur sources confirm typical double bond reactivity.

Introduction

Molecules with multiple bonds between heavier p-block elements continue to attract considerable interest in recent years due to their peculiar geometric and electronic structures and the ensuing high reactivity.^[1] The pioneering work by West (Si=Si), Yoshifuji (P=P), Brook (Si=C), and Becker (P=C) refuted the classical “double-bond” rule about the inability of p-block elements beyond the 2nd row of the periodic table to engage in multiple bonding.^[2] Since then, various compounds with homo- and heteronuclear multiple bonds between heavier elements from Group 13 to 15 have been isolated taking advantage of kinetic stabilization by sterically encumbering substituents.^[1,3] Such alkene and alkyne analogues can mimic the behavior of transition metals in activating unreactive small molecules and potentially catalyzing their conversion to value-added products due to the energetically accessible frontier orbitals of suitable symmetry.^[4]

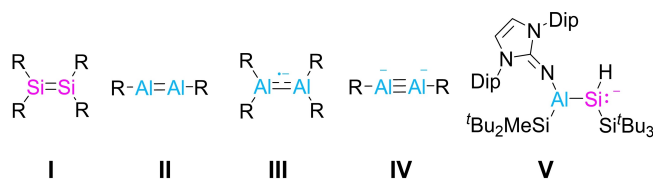
Of particular interest in this regard, the inherent electron-deficiency of Group 13 elements accounts for lower LUMO energies opening additional pathways for substrate interaction and general reactivity. In contrast to the extensively studied disilenes with Si=Si bond **I**^[3,5] (including functionalized derivatives as, for instance, disilenides^[5c,d,6]), however, dialumenes **II** have only been reported as Lewis acid-base adducts with electron-donors.^[7] Alternatively, the injection of electrons by reduction can diminish the inherent electron deficit of aluminum as shown by the isolation of dialumane radical monoanions **III**^[8] and a dialumene dianion **IV**.^[9] The latter concept has recently been employed by Inoue et al. for the synthesis of an alleged aluminatasilene, a compound with anticipated Al=Si bond, but all empirical and computational data rather supported the description as alumanyl silanide **V** (Scheme 1) with only very little double bond character.^[10] This was attributed by the authors to the more metallic and hence electropositive nature of aluminum as compared to silicon. We reasoned that the considerable π -backdonation from an N-heterocyclic imine substituent in Inoue’s alumanyl silanide of type **V** may also be detrimental to a substantial Al–Si π -interaction and therefore turned our attention to an aryl-substituted system. Previous reports by the Sekiguchi group and ourselves demonstrated the Si=Si bond of disilenides such as **1** can be converted into heteronuclear double bonds Si=E by treatment with suitable electrophiles and without an explicit reduction step (E = C, Ge, P).^[11]

Herein, expanding this approach to an aluminum-centered electrophile, we disclose the synthesis and isolation of an aluminatasilene with an authentic Al=Si bond. Structural, spectroscopic, and computational data suggest a pronounced double bond character due to its incorporation into an AlSi_3 four-membered ring, which is further supported by the characteristic intramolecular reactivity toward C–H bonds and the chalcogenation with sulfur or a sulfur transfer reagent.

[*] Dr. N. Parvin, Ankur, Prof. Dr. D. Scheschkewitz
 Krupp-Chair for General and Inorganic Chemistry
 Saarland University
 66123 Saarbrücken, Germany
 E-mail: scheschkewitz@mx.uni.saarland.de

Dr. B. Morgenstern
 Service Center X-ray diffraction
 Saarland University
 66123 Saarbrücken, Germany

© 2025 The Author(s). Angewandte Chemie International Edition published by Wiley-VCH GmbH. This is an open access article under the terms of the Creative Commons Attribution License, which permits use, distribution and reproduction in any medium, provided the original work is properly cited.



Scheme 1. Reported Al/Si multiple bond motifs **I** to **IV** (R = aryl, silyl, etc.) and Inoue’s alumanyl silanide **V**.

Results and Discussion

H_2AlCl is known as a convenient electrophilic precursor for the synthesis of novel aluminum compounds^[12] and easily prepared from the 1:1 reaction of AlCl_3 and LiAlH_4 .^[12a] The reaction of disilenide $\mathbf{1}\cdot[\text{Li}(\text{dme})_2]$ ^[13] with 1.1 equivalents of freshly prepared H_2AlCl , however, led to an intractable mixture of products, which we speculated to be due to secondary reactions of initial products with the aluminum reagent.

We therefore sought to test the early phases of the reaction by applying a 2:1 stoichiometry of $\mathbf{1}\cdot[\text{Li}(\text{dme})_2]$ and H_2AlCl . Indeed, the presence of a second equivalent of $\mathbf{1}\cdot[\text{Li}(\text{dme})_2]$ allowed for the trapping of the unidentified initial product and furnished a mixture containing an anionic Si_3Al cycle with a suspected $\text{Si}=\text{Al}$ bond according to a preliminary X-ray diffraction study that, however, suffered from severe disorder problems.

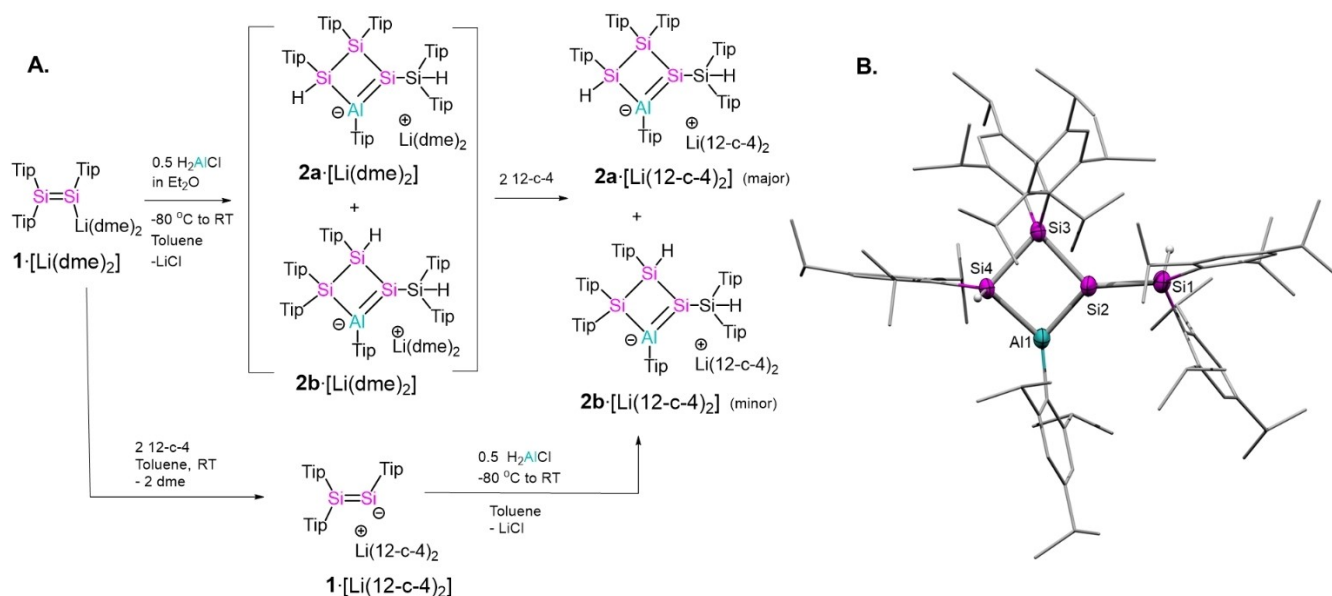
In order to improve the quality of crystals, we resorted to the preparation of solvent-separated ion pairs. Indeed, the addition of 2 eq. of 12-crown-4 to the reaction mixture afforded dark red crystals of $\mathbf{2a}\cdot[\text{Li}(12\text{-c-}4)_2]$ (40%) as the first fraction (Scheme 2A). As second fraction, orange-colored $\mathbf{2b}\cdot[\text{Li}(12\text{-c-}4)_2]$ (10%) is obtained alongside a small amount of residual $\mathbf{2a}\cdot[\text{Li}(12\text{-c-}4)_2]$. In the absence of air and moisture, both products are stable at room temperature in the solid state and in solution. Alternatively, compounds $\mathbf{2a}\cdot[\text{Li}(12\text{-c-}4)_2]$ and $\mathbf{2b}\cdot[\text{Li}(12\text{-c-}4)_2]$ can also be prepared by treatment of isolated $\mathbf{1}\cdot[\text{Li}(12\text{-c-}4)_2]$ with 0.5 eq. of H_2AlCl at -80°C (see Supporting Information for details).

The $^{29}\text{Si}\{^1\text{H}\}$ NMR spectrum of $\mathbf{2a}\cdot[\text{Li}(12\text{-c-}4)_2]$ shows four signals at -26.0 , -39.0 , -56.5 , and -57.1 ppm

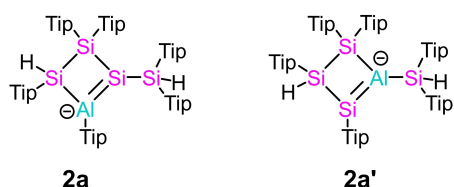
confirming that both equivalents of disilenide are incorporated in the product. All resonances are strongly upfield-shifted compared to $\mathbf{1}\cdot[\text{Li}(\text{dme})_2]$ ^[13] and $\mathbf{1}\cdot[\text{Li}(12\text{-c-}4)_2]$. The resonances at -56.5 and -57.1 ppm are assigned to the tertiary $\text{Si}-\text{H}$ moieties by 2D $^1\text{H}/^{29}\text{Si}$ correlation NMR spectroscopy. Two corresponding ^1H NMR singlets with ^{29}Si satellites are observed at 5.60 ($^1J_{\text{Si-H}} = 160.3$ Hz) and 6.08 ($^1J_{\text{Si-H}} = 175.4$ Hz) ppm. The ^{29}Si resonance at -39.0 ppm corresponds to a Si atom without directly bonded Tip group based on the absence of a crosspeak in the 2D $^1\text{H}/^{29}\text{Si}$ correlation NMR spectrum, which served as a first indication for the migration of one of the Tip groups to aluminum. For $\mathbf{2b}\cdot[\text{Li}(12\text{-c-}4)_2]$, four rather similar ^{29}Si resonances are found at -26.4 , -30.2 , -55.1 , and -60.3 ppm.

Single crystals of $\mathbf{2a}\cdot[\text{Li}(12\text{-c-}4)_2]$ were grown from a THF-hexane mixture (1:3).^[14] The compound crystallizes in the triclinic space group $P\bar{1}$ with the solvent-separated $[\text{Li}(12\text{-c-}4)_2]^+$ and one molecule of hexane. The molecular structure in the solid state (Scheme 2B) confirms the presence of a nearly planar four-membered AlSi_3 ring system (sum of internal bond angles 356.2°). In line with the conclusions drawn from the NMR data, the comparison of the bond lengths revealed that the Tip group of one of the former SiTip moieties had shifted to the newly introduced aluminum center. Hirshfeld tests confirm the assignment of Al1 and Si2.

The difference electron density map of an alternative refinement as position isomer $\mathbf{2a}'\cdot[\text{Li}(12\text{-c-}4)_2]$ (Scheme 3) indeed reveals pronounced mismatches between F_o and F_c (see Supporting Information). Reflecting the difference in covalent radii of Si and Al,^[15] the relatively unencumbered Al1 bonds to Si4 with an $\text{Al}-\text{Si}$ distance of $2.424(2)$ Å, while



Scheme 2. Synthesis and molecular structure of aluminatasilene. **A.** Synthesis of aluminatasilenes $\mathbf{2a}\cdot[\text{Li}(12\text{-c-}4)_2]$ and $\mathbf{2b}\cdot[\text{Li}(12\text{-c-}4)_2]$ from $\mathbf{1}\cdot[\text{Li}(\text{dme})_2]$ (Tip = 2,4,6-*i*-Pr₃C₆H₂, dme = 1,2-dimethoxyethane; 12-c-4 = 12-crown-4). **B.** Molecular structure of the anionic part of $\mathbf{2a}\cdot[\text{Li}(12\text{-c-}4)_2]$ in the solid state. Hydrogen atoms and co-crystallized solvent molecules (hexane) are omitted for clarity. Thermal ellipsoids at 50% probability. Selected bond lengths (Å) and bond angles ($^\circ$) of $\mathbf{2a}\cdot[\text{Li}(12\text{-c-}4)_2]$: Al1-Si2 2.283(1), Al1-Si4 2.424(1), Si1-Si2 2.344(1), Si2-Si3 2.351(1), Si3-Si4 2.425(1); Si2-Al1-Si4 86.65(5), Al1-Si2-Si3 94.91(4), Al1-Si4-Si3 89.53(4), Si2-Si3-Si4 85.13(4), Al1-Si2-Si1 131.49(6).



Scheme 3. Two possible isomers with Al=Si bond, **2a** and **2a'** (Tip = 2,4,6-*i*-Pr₃C₆H₂).

the single bond lengths of Si2 are 2.344(1) and 2.351(2) Å to Si1 and Si3, respectively. The bond length of Al1 to the *ipso*-carbon atom (C16) is 1.965(5) Å; the carbon atoms attached to silicon (C1, C31, C46, C61, C76) show somewhat smaller distances between 1.922(3) and 1.952(2) Å, despite evidently higher steric encumbrance. Cui et al. reported an Al-C_{Tip} bond length of 1.955(2) Å for a R₂Si₂AlTip ring with R being N-heterocyclic boryl substituents.^[16] The few reported cases of Tip group transfer in main group chemistry occurred to electron-deficient moieties.^[17]

Notably, the Al1-Si2 bond length in **2a**[Li(12-c-4)₂] of 2.283(1) Å is much shorter than that in Inoue's recently reported alumanyl silanide **V** (2.387(1) to 2.417(1) Å).¹⁰ The Al-Si bond length is closer to the sum of covalent radii for Al=Si (2.20 Å) than to that of Al-Si single bonds (2.42 Å), which clearly suggests a strongly polarized Al=Si double bond. It is also significantly shorter than the partially delocalized Al-Si bond lengths of Cui's cyclically delocalized Si₂Al three-membered rings (2.319(6) to 2.351(1) Å)^[16] and thus represents the shortest experimentally determined Al-Si bond reported to date. The double bond adopts a considerably *trans*-bent and twisted geometry with $\theta = 40.3(1)^\circ$ at Al1, $\theta = 21.7(6)^\circ$ at Si2 and a twist angle of $\tau = 23.0^\circ$. The bond from aluminum to the adjacent saturated silicon atom is considerably longer (Al1-Si4 2.424(2) Å) and in the range of reported sp² Al-Si single bond lengths.^[10,15] The Si-Si distances (Si2-Si3 2.351(2) Å, Si3-Si4 2.425(2) Å, Si1-Si2 2.344(1) Å) are in the range of Si-Si single bond lengths as well.^[15] The transannular distances of Al1...Si3 and Si2...Si4 are 3.414(1) and 3.231(1) Å, respectively, suggesting little if any interactions across the ring. The Al center in **2a**[Li(12-c-4)₂] is well-separated by 12.474(7) Å from the lithium cation due to coordination of two molecules of 12-crown-4. Since the Al=Si bond of **2b**[Li(12-c-4)₂] and consequently also the endocyclic Si-H moiety are disordered over two positions in the solid state, we refrain from a discussion of bonding parameters.

To get deeper insight into the electronic structure of anionic **2a**, we performed density functional theory (DFT) calculations at the B3LYP-D3BJ/def2SVP level of theory, including the isomeric **2a'** for comparison (Scheme 3). In order to minimize the use of computational resources, the *para*-isopropyl groups of the Tip substituents were replaced by methyl groups resulting in the simplified models **2a-mod** and **2a'-mod**, respectively. The optimized geometry of **2a-mod** reproduces the experimental solid-state structure much better than its position isomer **2a'-mod** with excellent agreement of bond lengths and bond angles of the AlSi₃ ring

(Supporting Information, Figure S36). Additionally, the Gibbs enthalpy of **2a-mod** is 5.72 kcal mol⁻¹ lower than that of **2a'-mod**. The highest occupied molecular orbital (HOMO) of **2a-mod** clearly corresponds to the Al-Si π -bond, whereas the HOMO-1 represents the σ -bond system of the AlSi₃ ring with some contribution from the π -system of the Tip groups attached to the silicon centers (Figure 1). The LUMO shows only an approximate correspondence to the π^* -orbital of Al=Si bond, possibly due to severe admixture of π orbitals of the Tip groups (Figure 1) and/or the polarization of the Al-Si bond apparent from the HOMO. Natural bond orbital (NBO) analysis indeed reveals that the π -bond is polarized toward the Si center involving 23.0% Al and 77.0% Si as expected on grounds of silicon's higher electronegativity. The electron occupancies of the Al-Si σ - and π -bonds are 1.94 and 1.73, respectively (see Supporting Information for details, Table S9). The natural population analysis (NPA) charges for the Al and Si centers are 0.90 and -0.72, respectively, suggesting a slightly less electropositive nature of aluminum than in **V** (Al: 1.03 and 1.25). The Wiberg bond index (WBI) of **2a-mod** is 1.31 (see Supporting Information for details, Table S9) and thus significantly higher than reported alumanyl silanide **V** (0.95 to 1.06) and a good match with theoretically calculated aluminatasilene ([H₂Al=SiH₂]⁻ = 1.40) and alumasilene (HAl=SiH₂: 1.41),¹⁰ which provides further strong support for the presence of an authentic Al=Si double bond in **2a**[Li(12-c-4)₂] rather than an alumanyl silanide as in **V**.

The UV/Vis spectrum of compound **2a**[Li(12-c-4)₂] exhibits the longest wavelength absorption at $\lambda_{\max} = 456$ nm ($\epsilon = 7939$ L mol⁻¹ cm⁻¹) in THF. TD-DFT calculations of **2a-mod** give a slightly more red-shifted absorption at $\lambda_{\max} = 488$ nm, which is attributed almost exclusively (94%) to the HOMO-LUMO transition (Supporting Information, Table S10 and S11). The admixture of several other absorptions at smaller wavelengths, however, shifts the resulting peak to the blue, closer to the experimental value (Supporting Information, Figure S38). The opposite applies to the second intense absorption band at $\lambda_{\max, \text{exp}} = 408$ nm ($\lambda_{\max, \text{cal}} = 377$ nm) ($\epsilon = 6976$ L mol⁻¹ cm⁻¹), which mainly corresponds

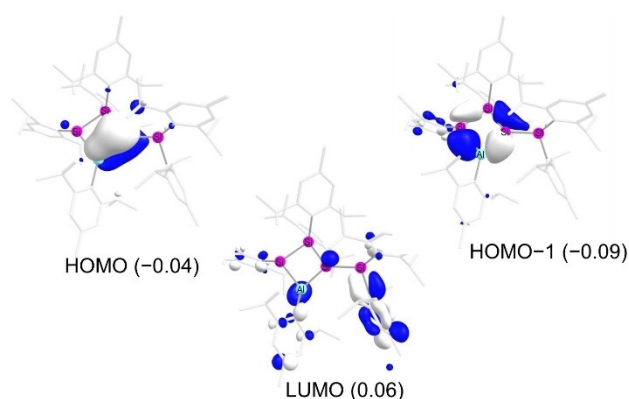
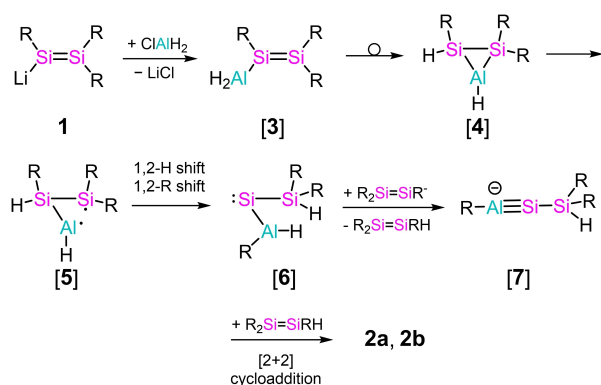


Figure 1. Selected frontier orbitals of **2a-mod** (energy in eV, contour value = 0.04; *para*-isopropyl groups of the Tip substituents are replaced by methyl groups).

to the HOMO to LUMO+11 and HOMO to LUMO+12 transition but is red-shifted by other contributing transitions.

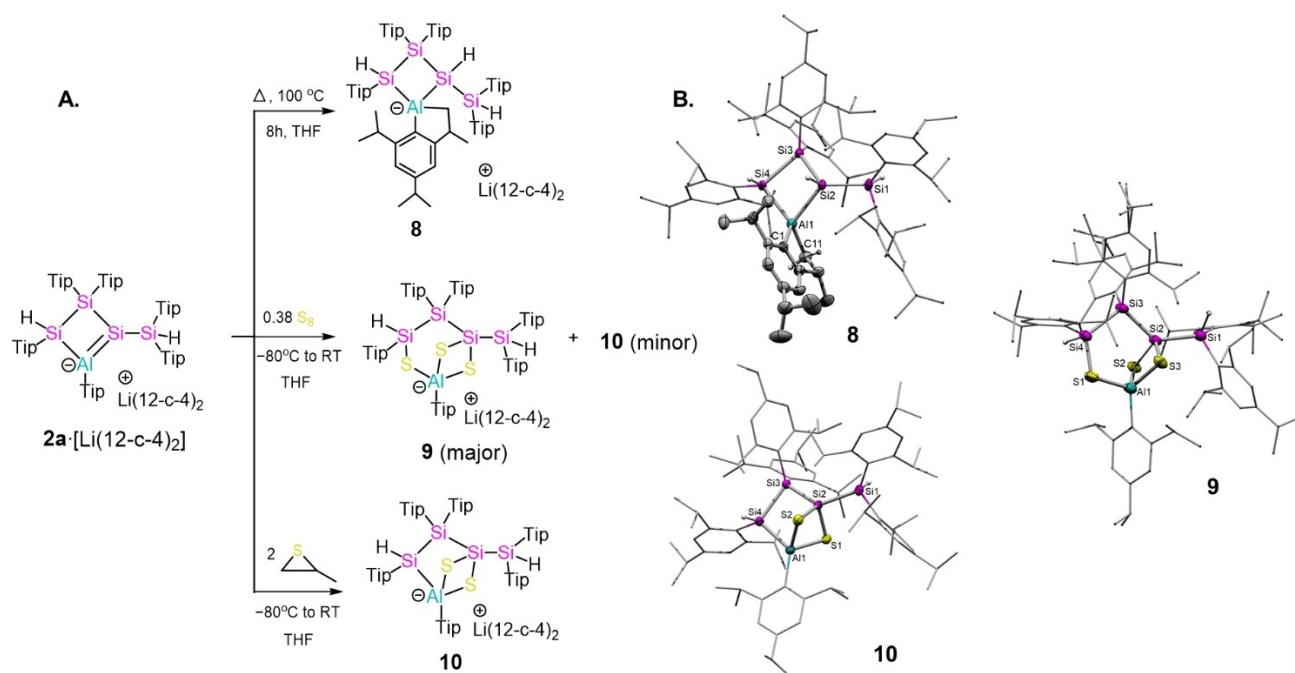
Due to the complexity of the system, we can only speculate about the formation mechanism of **2a** and **2b**, but the occurrence of the two regioisomers strongly suggests a [2+2] cycloaddition or similar as the final step. On this basis, we propose an initial nucleophilic substitution at H₂AlCl by the first equivalent of disilene **1** (Scheme 4). In view of the



Scheme 4. Proposed mechanism for the formation of **2a** and **2b** (Tip = 2,4,6-*i*Pr₃C₆H₂).

previously reported formation of three-membered rings from functionalized disilenes,^[18] the resulting alumanyl disilene **3** can reasonably be expected to cyclize to a strained alumadisilirane **4**. According to recent computations by Plannels and Espinosa Ferao,^[19] the combination of aluminum and silicon is expected to afford three-membered rings figuring among the most strained. Cleavage of the sterically more encumbered Al–Si bond would then lead to a highly reactive 1,3-diradical **5**, which could plausibly stabilize by a consecutive 1,2-hydrogen and aryl shifts to give alumanyl silylene **6**. The second equivalent of disilene **1** may then deprotonate at the aluminum center to give aluminatasilyne **7**, which would afford **2a** and **2b** by the aforementioned [2+2] cycloaddition.

Compound **2a**·[Li(12-*c*-4)₂] is thermally unstable and it starts to degrade at 80 °C. To investigate the thermally decomposed product, a THF solution of **2a**·[Li(12-*c*-4)₂] was heated at 100 °C for 8 h and an intramolecular C–H activation product is observed by ¹H and ²⁹Si NMR. Evaporation of THF afforded **8** as a yellow solid in 73 % yield (Scheme 5A). The ²⁹Si{¹H} NMR spectrum shows four signals at –24.2, –56.9, –71.4 and –91.3 ppm, which are slightly upfield-shifted compared to those of **2a**·[Li(12-*c*-4)₂]. The 2D ¹H/²⁹Si correlation NMR spectrum suggests the presence of three Si–H bonds. In the ¹H NMR spectrum,



Scheme 5. Reactivity of **2a**·[Li(12-*c*-4)₂] and molecular structure of the reaction products. **A.** Reactivity of **2a**·[Li(12-*c*-4)₂] by heating and with S₈ and propylene sulfide to synthesize **8**, **9** and **10**, respectively; Tip = 2,4,6-*i*Pr₃C₆H₂. **B.** Molecular structure of the anionic part of **8**, **9** and **10** in the solid state. Hydrogen atoms and co-crystallized solvent molecules (THF and hexane for **8**, hexane for **9** and **10**) are omitted for clarity. Thermal ellipsoids at 50% probability. Selected bond lengths (Å) and bond angles (°) of **8**: Al1–Si2 2.505(9), Al1–Si4 2.519(8), Si1–Si2 2.376(8), Si2–Si3 2.395(8), Si3–Si4 2.434(8), Al1–C11 1.998(2), Al1–C1 2.009(2); Si2–Al1–Si4 80.32(3), Al1–Si2–Si3 95.29(3), Si2–Si3–Si4 84.29(3), Al1–Si4–Si3 93.94(3), Al1–Si2–Si1 129.67(3). Selected bond lengths (Å) and bond angles (°) of **9**: Si1–Si2 2.387(3), Si2–Si3 2.394(2), Si3–Si4 2.501(4), Si4–S1 2.128(4), S1–Al1 2.267(3), Al1–S2 2.273(3), Al1–S3 2.280(3), Si2–S2 2.124(2), Si2–S3 2.134(2); Si2–Si3–Si4 101.84(1), Si3–Si4–S1 120.6(2), Si4–S1–Al1 107.05(1), S1–Al1–S2 110.24(1), S1–Al1–S3 103.40(1), Al1–S2–Si2 80.32(9), Al1–S3–Si2 79.95(9). Selected bond lengths (Å) and bond angles (°) of **10**: Si1–Si2 2.377(9), Si2–Si3 2.422(9), Si3–Si4 2.448(9), Al1–Si4 2.468(1), Si2–S1 2.143(9), Si2–S2 2.151(9), Al1–S1 2.333(1), Al1–S2 2.272(1); Si2–Si3–Si4 88.47(3), Si4–Al1–S1 90.15(3), Si4–Al1–S2 101.71(4), Al1–S1–Si2 77.19(3), Al1–S2–Si2 78.33(3).

two doublets with ^{29}Si satellites at 3.75 ($^1J_{\text{Si,H}} = 129.6$ Hz, $^3J_{\text{H,H}} = 6.5$ Hz) and 5.72 ppm ($^1J_{\text{Si,H}} = 174.7$ Hz, $^3J_{\text{H,H}} = 6.5$ Hz) correspond to two adjacent Si–H moieties. Another Si–H signal is observed at 5.32 ppm as a singlet with the obligatory satellites ($^1J_{\text{Si,H}} = 146.0$ Hz; see Supporting Information for details).

Single crystals of **8** suitable for X-ray analysis were obtained from a 1:1 THF-hexane mixture.^[14] The C–H activation product **8** crystallizes in the monoclinic space group $P2_1/c$ together with one molecule each of THF and hexane. The molecular structure of **8** in the solid state revealed the presence of a spirocyclic entity composed of a four-membered AlSi_3 ring, slightly distorted from planarity (sum of inner angles 353.8°), and a five-membered ring resulting from the addition of a methyl C–H bond of the Tip group at the Al center across the Al–Si double bond (Scheme 5B). Hence, the Al1–Si2 distance (2.505(9) Å) in **8** is much elongated compared to **2a**·[Li(12-c-4)₂] and similar to the Al1–Si4 bond length (2.519(8) Å) indicating the consumption of the Al=Si double bond. This type of intramolecular methyl C–H bond activation is commonly observed for multiply bonded and low-valent main group systems.^[20]

The presence of Al=Si double bond in **2a**·[Li(12-c-4)₂] is also reflected in its intermolecular reactivity. Treatment of **2a**·[Li(12-c-4)₂] with S_8 (0.38 eq.) in THF furnished an inseparable mixture of **9** (major) and **10** (minor) (Scheme 5A). The Iwamoto and Sekiguchi groups independently reported similar reactivity patterns with S_8 for B=Si double bonds.^[21] In order to increase the selectivity of the reaction, we employed propylene sulfide as a reagent, which is known for the stoichiometric transfer of sulfur to multiple bonds between heavier main group elements.^[17a,22] Indeed, the reaction of **2a**·[Li(12-c-4)₂] with 2 eq. of propylene sulfide in THF affords **10** exclusively. Notably, unlike elemental sulfur, the excess addition of propylene sulfide fails to generate **9**. The presence of two Si–H moieties in **10** is confirmed by corresponding signals in the ^1H (5.22 ppm, $^1J_{\text{Si,H}} = 156.1$ Hz; 5.74 ppm, $^1J_{\text{Si,H}} = 175.4$ Hz) and ^{29}Si NMR spectra (–55.8 and –69.9 ppm). In case of **9**, two Si–H peaks are observed as singlets with ^{29}Si satellites at 7.01 ($^1J_{\text{Si,H}} = 206.7$ Hz) and 5.72 ($^1J_{\text{Si,H}} = 178.0$ Hz) ppm and the corresponding ^{29}Si peaks at –25.2 and –51.3 ppm.

Colorless and pale yellow crystals of **9** and **10**, respectively, were grown as a mixture from the reaction of **2a**·[Li(12-c-4)₂] with S_8 in 1:1 THF-hexane solution,^[14] but the structure of **10** could not be refined satisfactorily due to the heavy disorder. Better single crystals of **10** were obtained from the reaction of **2a**·[Li(12-c-4)₂] with propylene sulfide, grown from a 1:1 THF-hexane mixture. The products **9** and **10** crystallize in monoclinic space groups Cc (**9**) and $P2_1/n$ (**10**). The X-ray diffraction studies confirm the formation of four-membered AlSi_2Si dithiacycles in both cases, resulting from the addition of two sulfur atoms to the Al=Si bond (Scheme 5B). While in case of **10**, a bicyclo-[2.1.1]hexane derivative is formed, an additional sulfur atom is inserted into the adjacent Al1–Si4 single bond to generate the unique AlSi_3S_3 bicyclo[3.1.1]heptane structure of **9**. Al and Si atoms of **9** and **10** are four-coordinate and adopt

distorted tetrahedral coordination environments. As expected, the Al–S (between 2.267(3) and 2.333(1) Å) and Si–S distances (between 2.124(3) and 2.151(9) Å) are in the range of single bonds.

Conclusion

In conclusion, we prepared the first bona fide example of a Al=Si double bond taking advantage of its incorporation into a strained small cyclic system and the presence of bulky substituents. X-ray diffraction on single crystals of **2a**·[Li(12-c-4)₂] confirms the shortest Al–Si bond length reported to date and computational studies further support the Al–Si π -bond character. Thermally unstable **2a**·[Li(12-c-4)₂] rearranges upon heating as the Al=Si double bond activates the relatively inert C(sp³)-H bond of the adjacent Tip group. Further support for the presence of an Al=Si bond is garnered from the reactions of **2a**·[Li(12-c-4)₂] with elemental sulfur and propylene sulfide resulting in 1,3-dithiacycles. Clearly, **2a**·[Li(12-c-4)₂] offers significant potential to explore the Al=Si reactivity towards small molecules and corresponding investigations are currently underway in our laboratory.

Supporting Information

The authors have cited additional references within the Supporting Information.^[12a,13,23–32]

Acknowledgements

This work was supported by the Alexander von Humboldt Foundation (Research Fellowship for N.P.). We thank Prof. Stella Stopkowicz for access to the computational clusters. We also acknowledge the instrumentation facilities provided by the service center for X-ray analysis established with the financial support from the Saarland University and the Deutsche Forschungsgemeinschaft (INST 256/506-1). Open Access funding enabled and organized by Projekt DEAL.

Conflict of Interest

The authors declare no conflict of interest.

Data Availability Statement

The data that support the findings of this study are available in the supplementary material of this article.

Keywords: aluminium · silicon · double bond · strained four-membered ring

- [1] a) P. P. Power, *Chem. Rev.* **1999**, *99*, 3463–3504; b) R. C. Fischer, P. P. Power, *Chem. Rev.* **2010**, *110*, 3877–3923; c) P. P. Power, *Organometallics* **2020**, *39*, 4127–4138; d) D. J. Liptrout, P. P. Power, *Nat. Rev. Chem.* **2017**, *1*, 0004.
- [2] a) R. West, M. J. Fink, *Science* **1981**, *214*, 1343–1344; b) M. Yoshifuji, I. Shima, N. Inamoto, K. Hirotsu, T. Higuchi, *J. Am. Chem. Soc.* **1981**, *103*, 4587–4589; c) A. G. Brook, F. Abdesaken, B. Gutekunst, G. Gutekunst, R. K. Kallury, *J. Chem. Soc., Chem. Commun.* **1981**, 191–192; d) G. Becker, G. Gresser, W. Uhl, *Z. Naturforsch. B* **1981**, *36*, 16–19.
- [3] a) V. Y. Lee, A. Sekiguchi, J. Escudí, H. Ranaivonjatovo, *Chem. Lett.* **2010**, *39*, 312–318; b) P. P. Power, *Chem. Commun.* **2003**, 2091–2101; c) C. Weetman, *Chem. Eur. J.* **2021**, *27*, 1941–1954; d) V. Y. Lee, A. Sekiguchi, *Organometallic Compounds of Low-Coordinate Si, Ge, Sn and Pb: From Phantom Species to Stable Compounds*, J. Wiley & Sons, Ltd, Chichester, **2010**; e) M. Kira, T. Iwamoto, *Adv. Organomet. Chem.* **2006**, *54*, 73–148; f) R. Okazaki, R. West, *Adv. Organomet. Chem.* **1996**, *39*, 231–278.
- [4] a) P. P. Power, *Nature* **2010**, *463*, 171–177; b) C. Weetman, S. Inoue, *ChemCatChem* **2018**, *10*, 4213–4228.
- [5] a) R. West, *Polyhedron* **2002**, *21*, 467–472; b) F. Hanusch, L. Groll, S. Inoue, *Chem. Sci.* **2021**, *12*, 2001–2015; c) A. Rammo, D. Scheschkewitz, *Chem. Eur. J.* **2018**, *24*, 6866–6885; d) C. Präsang, D. Scheschkewitz, *Chem. Soc. Rev.* **2016**, *45*, 900–921; e) T. Iwamoto, S. Ishida, *Struct. Bond.* **2013**, *156*, 125–202.
- [6] a) D. Scheschkewitz, *Chem. Lett.* **2011**, *40*, 2–11; b) D. Scheschkewitz, *Chem. Eur. J.* **2009**, *15*, 2476–2485.
- [7] a) P. Bag, A. Porzelt, P. J. Altmann, S. Inoue, *J. Am. Chem. Soc.* **2017**, *139*, 14384–14387; b) R. L. Falconer, K. M. Byrne, G. S. Nichol, T. Krämer, M. J. Cowley, *Angew. Chem.* **2021**, *133*, 24907–24913; *Angew. Chem. Int. Ed.* **2021**, *60*, 24702–24708; c) C. Weetman, A. Porzelt, P. Bag, F. Hanusch, S. Inoue, *Chem. Sci.* **2020**, *11*, 4817–4827.
- [8] a) C. Luta, K. R. Pörschke, C. Krüger, K. Hildenbrand, *Angew. Chem.* **1993**, *105*, 451–453; *Angew. Chem. Int. Ed.* **1993**, *32*, 388–390; b) R. J. Wehmschulte, K. Ruhlandt-Senge, M. M. Olmstead, H. Hope, B. E. Sturgeon, P. P. Power, *Inorg. Chem.* **1993**, *32*, 2983–2984; c) W. Uhl, A. Vester, W. Kaim, J. Poppe, *J. Organomet. Chem.* **1993**, *454*, 9–13.
- [9] R. J. Wright, M. Brynda, P. P. Power, *Angew. Chem.* **2006**, *118*, 6099–6102; *Angew. Chem. Int. Ed.* **2006**, *45*, 5953–5956.
- [10] M. Ludwig, D. Franz, A. E. Ferao, M. Bolte, F. Hanusch, S. Inoue, *Nature Chem.* **2023**, *15*, 1452–1460.
- [11] a) I. Bejan, D. Güclü, S. Inoue, M. Ichinohe, A. Sekiguchi, D. Scheschkewitz, *Angew. Chem.* **2007**, *119*, 3413–3416; *Angew. Chem. Int. Ed.* **2007**, *46*, 3349–3352; b) I. Bejan, S. Inoue, M. Ichinohe, A. Sekiguchi, D. Scheschkewitz, *Chem. Eur. J.* **2008**, *14*, 7119–7122; c) S. Inoue, M. Ichinohe, A. Sekiguchi, *Angew. Chem.* **2007**, *119*, 3410–3412; *Angew. Chem. Int. Ed.* **2007**, *46*, 3346–3348; d) P. Willmes, M. J. Cowley, M. Hartmann, M. Zimmer, V. Huch, D. Scheschkewitz, *Angew. Chem.* **2014**, *126*, 2248–2252; *Angew. Chem. Int. Ed.* **2014**, *53*, 2216–2220; e) A. Jana, M. Majumdar, V. Huch, M. Zimmer, D. Scheschkewitz, *Dalton Trans.* **2014**, *43*, 5175–5181; f) Y. Heider, P. Willmes, D. Mühlhausen, L. Klemmer, M. Zimmer, V. Huch, D. Scheschkewitz, *Angew. Chem.* **2019**, *131*, 1958–1964; *Angew. Chem. Int. Ed.* **2019**, *58*, 1939–1944.
- [12] a) M. Zhong, Y. Liu, S. Kundu, N. Graw, J. Li, Z. Yang, R. Herbst-Irmer, D. Stalke, H. W. Roesky, *Inorg. Chem.* **2019**, *58*, 10625–10628; b) C. Ganesamoorthy, S. Loerke, C. Gemel, P. Jerabek, M. Winter, G. Frenking, R. A. Fischer, *Chem. Commun.* **2013**, *49*, 2858–2860; c) S. G. Alexander, M. L. Cole, M. Hilder, J. C. Morris, J. B. Patrick, *Dalton Trans.* **2008**, 6361–6363.
- [13] D. Scheschkewitz, *Angew. Chem.* **2004**, *116*, 3025–3028; *Angew. Chem. Int. Ed.* **2004**, *43*, 2965–2967.
- [14] CCDC deposition numbers 2378776 (for **1**[Li(12-c-4)₂]), 2378777 (for **2a**[Li(12-c-4)₂]), 2378778 (for **2b**[Li(12-c-4)₂]), 2378779 (for **8**), 2378781 (for **9**), 2378780 (for **10**) contain the supplementary crystallographic data for this paper. These data are provided free of charge by the joint Cambridge Crystallographic Data Centre and Fachinformationszentrum Karlsruhe Access Structures service.
- [15] a) B. Cordero, V. Gómez, A. E. Platero-Prats, M. Revés, J. Echeverría, E. Cremades, F. Barragán, S. Alvarez, *Dalton Trans.* **2008**, 2832–2838; b) P. Pykkö, M. Atsumi, *Chem. Eur. J.* **2009**, *15*, 186–197.
- [16] L. Guo, J. Zhang, C. Cui, *J. Am. Chem. Soc.* **2023**, *145*, 27911–27915.
- [17] a) A. Sekiguchi, R. Izumi, V. Y. Lee, M. Ichinohe, *Organometallics* **2003**, *22*, 1483–1486; b) K. Abersfelder, A. Russell, H. S. Rzepa, A. J. P. White, P. R. Haycock, D. Scheschkewitz, *J. Am. Chem. Soc.* **2012**, *134*, 16008–16016.
- [18] a) K. Abersfelder, T. Nguyen, D. Scheschkewitz, *Z. Anorg. Allg. Chem.* **2009**, *635*, 2093–2098; b) K. Abersfelder, D. Scheschkewitz, *J. Am. Chem. Soc.* **2008**, *130*, 4114–4121; c) K. Abersfelder, D. Scheschkewitz, *Pure Appl. Chem.* **2010**, *82*, 595–602.
- [19] A. R. Planells, A. Espinosa Ferao, *Inorg. Chem.* **2022**, *61*, 13846–13857.
- [20] Selected examples: a) M. J. Fink, D. J. DeYoung, R. West, J. Michl, *J. Am. Chem. Soc.* **1983**, *105*, 1070–1071; b) P. Jutzi, C. Leue, *Organometallics* **1994**, *13*, 2898–2899; c) T. Nguyen, D. Scheschkewitz, *J. Am. Chem. Soc.* **2005**, *127*, 10174–10175; d) D. Reiter, R. Holzner, A. Porzelt, P. J. Altmann, P. Frisch, S. Inoue, *J. Am. Chem. Soc.* **2019**, *141*, 13536–13546; e) C. Shan, S. Yao, M. Driess, *Chem. Soc. Rev.* **2020**, *49*, 6733–6754; f) P. K. Majhi, M. Zimmer, B. Morgenstern, V. Huch, D. Scheschkewitz, *J. Am. Chem. Soc.* **2021**, *143*, 13350–13357; g) M. Frutos, N. Parvin, A. Baceiredo, D. Madec, N. Saffon-Merceron, V. Branchadell, T. Kato, *Angew. Chem. Int. Ed.* **2022**, *61*, e202201932; *Angew. Chem.* **2022**, *134*, e202201932.
- [21] a) N. Nakata, A. Sekiguchi, *Chem. Lett.* **2007**, *36*, 662–663; b) Y. Suzuki, S. Ishida, S. Sato, H. Isobe, T. Iwamoto, *Angew. Chem.* **2017**, *129*, 4664–4668; *Angew. Chem. Int. Ed.* **2017**, *56*, 4593–4597.
- [22] a) H. Zhao, L. Klemmer, M. J. Cowley, V. Huch, M. Zimmer, D. Scheschkewitz, *Z. Anorg. Allg. Chem.* **2018**, *644*, 999–1005; b) V. Y. Lee, S. Miyazaki, H. Yasuda, A. Sekiguchi, *J. Am. Chem. Soc.* **2008**, *130*, 2758–2759; c) V. Y. Lee, S. Miyazaki, H. Yasuda, A. Sekiguchi, *Phosphorus Sulfur Silicon Relat. Elem.* **2011**, *186*, 1346–1350; d) V. Y. Lee, O. A. Gapurenko, S. Miyazaki, A. Sekiguchi, R. M. Minyaev, V. I. Minkin, H. Gornitzka, *Angew. Chem.* **2015**, *127*, 14324–14328; *Angew. Chem. Int. Ed.* **2015**, *54*, 14118–14122.
- [23] G. R. Fulmer, A. J. M. Miller, N. H. Sherden, H. E. Gottlieb, A. Nudelman, B. M. Stoltz, J. E. Bercaw, K. I. Goldberg, *Organometallics* **2010**, *29*, 2176–2179.
- [24] G. M. Sheldrick, *Acta Cryst. A* **2015**, *71*, 3–8.
- [25] G. M. Sheldrick, *Acta Cryst. C* **2015**, *71*, 3–8.
- [26] C. B. Hübschle, G. M. Sheldrick, B. Dittrich, *J. Appl. Crystallogr.* **2011**, *44*, 1281–1284.
- [27] M. J. Frisch, G. W. Trucks, H. B. Schlegel, G. E. Scuseria, M. A. Robb, J. R. Cheeseman, G. Scalmani, V. Barone, G. A. Petersson, H. Li, X. Nakatsuji, M. Caricato, A. V. Marenich, J. Bloino, B. G. Janesko, R. Gomperts, B. Mennucci, H. P. Hratchian, J. V. Ortiz, A. F. Izmaylov, J. L. Sonnenberg, D. Williams-Young, F. Ding, F. Lipparini, F. Egidi, J. Goings, B. Peng, A. Petrone, T. Henderson, D. Ranasinghe, V. G. Zakrzewski, J. Gao, N. Rega, G. Zheng, W. Liang, M. Hada, M. Ehara, K. Toyota, R. Fukuda, J. Hasegawa, M. Ishida, T.

- Nakajima, Y. Honda, O. Kitao, H. Nakai, T. Vreven, K. Throssell, J. A. Montgomery, Jr., J. E. Peralta, F. Ogliaro, M. J. Bearpark, J. J. Heyd, E. N. Brothers, K. N. Kudin, V. N. Staroverov, T. A. Keith, R. Kobayashi, J. Normand, K. Raghavachari, A. P. Rendell, J. C. Burant, S. S. Iyengar, J. Tomasi, M. Cossi, J. M. Millam, M. Klene, C. Adamo, R. Cammi, J. W. Ochterski, R. L. Martin, K. Morokuma, O. Farkas, J. B. Foresman, D. J. Fox, Gaussian 16, Revision C.01, Gaussian, Inc., Wallingford CT, **2019**.
- [28] a) J. P. Perdew, *Phys. Rev. B* **1986**, *33*, 8822–8824; b) A. D. Becke, *Phys. Rev. A* **1988**, *38*, 3098–3100.
- [29] a) A. Schäfer, H. Horn, R. Ahlrichs, *J. Chem. Phys.* **1992**, *97*, 2571–2577; b) A. Schäfer, C. Huber, R. Ahlrichs, *J. Chem. Phys.* **1994**, *100*, 5829–5835; c) F. Weigend, R. Ahlrichs, *Phys. Chem. Chem. Phys.* **2005**, *7*, 3297–3305; d) F. Weigend, *Phys. Chem. Chem. Phys.* **2006**, *8*, 1057–1065.
- [30] S. Grimme, J. Antony, S. Ehrlich, H. J. Krieg, *Chem. Phys.* **2010**, *132*, 154104.
- [31] Chemcraft - graphical software for visualization of quantum chemistry computations. <https://www.chemcraftprog.com>.
- [32] E. D. Glendening, J. K. Badenhoop, A. E. Reed, J. E. Carpenter, F. Weinhold, NBO Version 3.1, Theoretical Chemistry Institute, University of Wisconsin, Madison, **2010**.

Manuscript received: November 12, 2024

Accepted manuscript online: February 5, 2025

Version of record online: February 13, 2025